Article

High Field X-ray Diffraction Study for Ni$_{46.4}$Mn$_{38.8}$In$_{12.8}$Co$_{2.0}$ Metamagnetic Shape Memory Film

Yoshifuru Mitsui [1],*, Keiichi Koyama [1], Makoto Ohtsuka [2], Rie Y. Umetsu [3], Ryosuke Kainuma [4] and Kazuo Watanabe [3]

[1] Graduate School of Science and Engineering, Kagoshima University, Kagoshima 890-0065, Japan; koyama@sci.kagoshima-u.ac.jp
[2] Institute of Multidisciplinary Research for Advanced Materials, Tohoku University, Sendai 980-8577, Japan; makoto.ohtsuka.d7@tohoku.ac.jp
[3] Institute for Materials Research, Tohoku University, Sendai 980-8577, Japan; rieume@imr.tohoku.ac.jp (R.Y.U.); kwata@imr.tohoku.ac.jp (K.W.)
[4] Graduate School of Engineering, Tohoku University, Sendai 980-8579, Japan; kainuma@material.tohoku.ac.jp
* Correspondence: mitsui@sci.kagoshima-u.ac.jp; Tel.: +81-99-285-8082

Abstract: The transformation behaviors on metamagnetic shape memory Ni$_{46.4}$Mn$_{38.8}$In$_{12.8}$Co$_{2.0}$ film were investigated by X-ray diffraction experiments in the temperature up to 473 K and magnetic fields $\mu_0 H$ up to 5 T. The prepared film showed the parent phase with L2$_1$ structure at 473 K, and with preferred orientation along the 111 plane. The magnetic field induced reverse transformation was directly observed at T = 366 K, which was just around the reverse transformation starting temperature.

1. Introduction

Ferromagnetic shape memory alloys (FSMAs) have been studied actively as high-performance actuator materials since a large magnetic field-induced strain of 0.2% was found in Ni$_2$MnGa alloys by Ullakko et al. [1]. That this large magnetic field induced strain in the ferromagnetic Ni$_2$MnGa single crystal is explained by the rearrangement of twin variants of martensitic phase (M-phase) [2]. To control the performance in Ni-Mn-Ga alloys (e.g., magnetic properties, martensitic transformation temperatures, etc.), they were examined by the substitution of the elements [3,4].

In 2004, Sutou et al. found that Ni-Mn-X (X = In, Sn, and Sb) alloys with Heusler-type structure showed a martensitic transformation with magnetic transition [5]. The magnetization of parent phase in Ni-Mn-X series shows large magnetization, whereas that of M-phase is small [5]. The Mössbauer spectroscopy studies on Fe^{57}-doped Ni-Mn-In and Ni-Mn-Sn systems found that the magnetism of the M-phase was paramagnetism [6,7]. The Co-doped Ni-Mn-In system was found to show a discontinuous jump in magnetization between P- and M-phase [8]. The strain of 3% was almost recovered by the application of a 7 T magnetic field, which was a so-called metamagnetic shape memory effect (MSM effect) [8]. An MSM effect was also found in Co-doped Ni-Mn-Sn alloys [9]. The crystal structure of M-phase in Ni-Co-Mn-In was reported to be the mixture of five- and seven-layered modulated monoclinic structure (10M and 14M) by electron microscopy observation [10]. Structural properties of Ni-Co-Mn-In bulk alloy were reported by using synchrotron radiation in high magnetic fields [11]. According to Reference [11], the crystal structure of M-phase was 14M. Additionally, field-induced reverse transformation under compression was observed in magnetic fields up to 5 T [11].

FSMAs films have been studied for the application as actuators [12–14]. Ni-Co-Mn-In MSM ribbons and films were also prepared by rapid solidification [15] and magnetron sputtering [16],

respectively. Recently, Ni-Co-Mn-In films were examined for the application for energy harvesting [17]. According to Reference [16], the annealing temperature changes the crystal structure of M-phases. Recent reports for the Ni-Co-Mn-In films show that as-deposited film shows body-centered cubic structure, whereas the modulated structure appeared after annealing [18]. According to the phase diagram of $Ni_{50-x}Mn_{37}In_{13}Co_x$ ribbon with 30 μm thick, the reverse transformation temperature changed by ~200 K in $0 \leq x \leq 9$, and had a cusp at $x \sim 3$ [15]. Furthermore, according to Reference [18], minor changes in compositions of the film also changed the transformation behavior of the films (e.g., transformation temperature and thermal hysteresis). Therefore, the transformation behaviors and crystal structures of MSM films were sensitive to slight composition change and the annealing conditions.

Although the annealing effects, microstructure, and martensitic transformation behaviors were evaluated for MSM films and ribbons, the martensitic transformation induced by magnetic fields has not yet been confirmed by using in-situ observation techniques.

The high field X-ray diffraction (HF-XRD) technique was one of the suitable methods for investigating the structural properties in magnetic field—particularly the field-induced structural transformations. So far, the relationship between magnetic transition and structural transformation was investigated for magnetic refrigerants by using HF-XRD [19–21]. In addition, HF-XRD study has also been carried out for FSMAs and MSM alloys such as Ni_2MnGa alloys [22], Ni-Mn-Sn alloy [23], and for Ni-Co-Mn-In alloy [24]. In 2008, HF-XRD for high temperatures was developed in temperatures up to 473 K [25]. Magnetic field-induced reverse transformations in $Ni_{40}Co_{10}Mn_{34}Al_{16}$ MSM alloys were observed at 408 K using this apparatus [26].

As described above, in this study, in order to observe field-induced reverse transformation in Co-doped Ni-Mn-In film, high field X-ray diffraction experiments were performed under magnetic fields up to 5 T and temperature ranging from 293 to 473 K.

2. Materials and Methods

Co-doped Ni-Mn-In films of 1 μm thickness were deposited on a poly-vinyl alcohol (PVA) substrate using a dual magnetron sputtering apparatus (CFS-4ES, Shibaura, Yokohama, Japan). The apparatus has radio-frequency (RF) and direct current (DC) power sources. The RF power for $Ni_{45}Mn_{40}In_{15}$ target was kept at 200 W and the DC power for Co target was kept at 5 W. After separating from the PVA substrate, the films were heat-treated at 1173 K for 3.6 ks. The chemical composition of the film was determined by an inductively coupled plasma (ICP) spectrometry apparatus (Optima 3300, Perkin Elmer Inc., Waltham, MA, USA). The composition of the sample was determined to be $Ni_{46.4}Mn_{38.8}In_{12.8}Co_{2.0}$. According to the reports about Ni-Co-Mn-In films [16,18], the transformation behavior was sensitive to the annealing condition, composition of Co, and so on. In this study, as described below, the transformation temperatures of $Ni_{46.4}Mn_{38.8}In_{12.8}Co_{2.0}$ films are above room temperature (RT), which is suitable for observing the structural change by HF-XRD system at high temperature.

The martensitic transformation temperatures M_s: martensitic transformation starting temperature, M_f: martensitic transformation finishing temperature, A_s: reverse transformation starting temperature, and A_f: reverse transformation finishing temperature were determined by the magnetization measurements by using a superconducting quantum interface device (SQUID) magnetometer in magnetic fields $\mu_0 H$ up to 5 T and the temperature T ranging from 10 to 390 K. The transformation temperatures are defined using the intersection of the base line and the tangent line with the largest slope in the thermomagnetization curve.

High field X-ray diffraction measurements using Cu Kα radiation were performed for $\mu_0 H \leq 5$ T and in the temperature range from 293 to 473 K under He atmosphere. Details of the HF-XRD setup are reported in Reference [25]. $Ni_{46.4}Mn_{38.8}In_{12.8}Co_{2.0}$ films were fixed with Apiezon H Grease &I Materials Ltd., Manchester, UK) on a copper sample holder. The surface of the film was parallel to the magnetic field, and was perpendicular to the scattering vector of X-ray.

3. Results and Discussion

Figure 1 shows the thermomagnetization curve for $Ni_{46.4}Mn_{38.8}In_{12.8}Co_{2.0}$ film in $\mu_0 H = 0.05$ T, 1 T, and 5 T. In all curves, metamagnetic phase transition from M- to P-phase is clearly observed. The transformation temperatures in $\mu_0 H = 1$ T were determined to be $M_s = 373$ K, $M_f = 355$ K, $A_s = 368$ K, and $A_f = 385$ K. Meanwhile, these temperatures at 5 T were obtained to be $M_s = 373$ K, $M_f = 352$ K, $A_s = 365$ K, and $A_f = 385$ K, which were slightly lower than that in 1 T. Figure 2 shows the *M–H* curve obtained at 348, 366, and 373 K, which were $T < A_s$, $T \sim A_s$, and $A_s < T < A_f$, respectively. *M–H* data were collected after the zero-field heating from $T < M_f$. The magnetization at 348 K is very small and almost independent of magnetic fields. At 366 K, the small jump in magnetization due to metamagnetic transition was observed for $\mu_0 H \geq 4$ T. On the other hand, the curve at 373 K showed large magnetization, and magnetic transition and hysteresis were not observed.
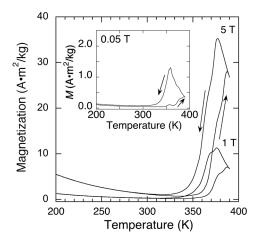

Figure 1. Thermomagnetization curves for $Ni_{46.4}Mn_{38.8}In_{12.8}Co_{2.0}$ film at $\mu_0 H = 1$ T and 5 T. The inset is the thermomagnetization curve obtained at $\mu_0 H = 0.05$ T.
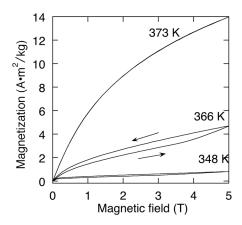

Figure 2. Isothermal magnetization curves for $Ni_{46.4}Mn_{38.8}In_{12.8}Co_{2.0}$ film at 348, 366, and 373 K. Each curve ware obtained after the zero field heating from $T > M_f$.

Figure 3 shows the XRD patterns for $Ni_{46.4}Mn_{38.8}In_{12.8}Co_{2.0}$ film at room temperature (RT) and at 473 K. The diffraction peaks at $2\theta \sim 43°$, $50°$, $74°$, and $90°$ belong to the copper sample holder. The other peaks at RT belong to the M-phase, which are indicated by the closed circles in Figure 3. The diffraction profile at 473 K is quite different from that at RT. The diffraction peaks at 473 K were indexed by $L2_1$ structure (hkl_P), which was P-phase. This profile shows the preferred orientation along (111) plane parallel to film surface. As described below, the lattice parameters of the P-phase were in good agreement with that of bulk Ni-Co-Mn-In samples. To compare the diffraction patterns of P- and

M-phase, 111_P, 220_P, and 222_P seem to split during transformation, indicating the decline of crystal symmetry. In this study, it is difficult to determine the crystal structure of M-phase because the P-phase shows preferred orientation. 14M and 10M structure did not represent the obtained XRD patterns. According to the reports for bulk Ni-Co-Mn-In sample, the crystal structure of M-phase is reported to be a mixture of 14M and 10M structures [10], or 14M structures [11]. Therefore, the crystal structure of M-phase in the film is considered to be a mixture of 10M and 14M or the related modulated structure.
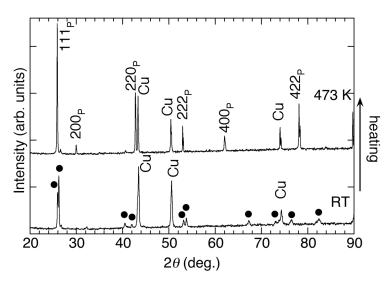

Figure 3. XRD pattern of $Ni_{46.4}Mn_{38.8}In_{12.8}Co_{2.0}$ film at room temperature (RT) and 473 K. hkl_A indicates the Miller indices of the $L2_1$ structure (parent phase). The closed circles are the diffraction peaks belonging to the martensitic phase.

Figure 4 shows the XRD patterns in the 2θ range from 52° to 55° at various temperatures in heating in a zero field (a), cooling in a zero field (b), heating in 5 T (c), and cooling in 5 T (d). In the heating process from 303 K in a zero field, the 222_P diffraction developed between 363 and 373 K. For $T \geq 383$ K, only the diffraction peak of $L2_1$ structure was observed. With decreasing T from 473 K, the peak intensity of 222_P diffraction began to suppress at $T = 363$ K, and the diffraction at $2\theta \sim 53.5°$ appeared, and the diffraction profile did not change below 353 K. On the other hand, as seen in Figure 4c,d, the change in diffraction profile was also observed with a slightly lower temperature region than that in a zero field. These transformation behaviors were consistent with the thermomagnetization curve shown in Figure 1. Using the diffraction profiles of Figure 4a,b, the lattice parameter a of $L2_1$ structure at room temperature was evaluated. Figure 5 shows the determined lattice parameter a in a zero field. The obtained lattice parameter and temperature show linear relation. The lattice parameter a at 300 K was obtained to be 0.597 nm, which is in good agreement with previous reports for bulk sample [8].

Figures 6 and 7 show the isothermal XRD patterns in magnetic fields up to 5 T at fixed temperature of 366 K and 371 K. The measurements were carried out after zero-field heating from room temperature ($T < M_f$). The diffraction peaks of M-phase (closed circles) and P-phase (222_P peak) were observed in all profiles. As seen in Figure 6, with applied magnetic field, the sharp peak belonging to the 222_P diffraction was induced at $2\theta \sim 53°$. Although 222_P diffraction was induced by the magnetic field, the reverse transformation from the M-phase to P-phase was incomplete at 5 T. With decreasing $\mu_0 H$ from 5 T to 0 T, the profile did not change efficiently. On the other hand, the diffraction peaks at 371 K of P-phase became stronger than 366 K, indicating the irreversibility of the field-induced transformation. On the other hand, as seen in Figure 7, the field-induced development of 222_P diffraction was not observed clearly.

Figure 8 shows the magnetic field dependence of the difference of peak intensity I_{P-M} between two peaks at $2\theta \sim 53°$ and $2\theta \sim 53.5°$. As described above, because the 222_P peak of P-phase and the peak

of M-phase overlapped at $2\theta \sim 53°$ and the peak at $53.5°$ only belonged to M-phase, enhancement of $I_{P\text{-}M}$ indicated the field-induced reverse transformation. $I_{P\text{-}M}$ gradually increased to 3 T. $I_{P\text{-}M}$ showed a jump for $\mu_0 H > 3$ T, and did not recover in decreasing $\mu_0 H$. This means that the magnetic-field-induced transformation was directly observed for $\mu_0 H > 3$ T. Isothermal diffraction pattern at 371 K also showed the increase of $I_{P\text{-}M}$ with increasing H. However, the increment of $I_{P\text{-}M}$ was obtained to be 25 count from $\mu_0 H = 0$ to 5 T, which was much smaller than 366 K. Thus, it was found that the field-induced transformation of the film exhibits a narrow temperature window. This transformation behavior was qualitatively consistent with the magnetization measurements.
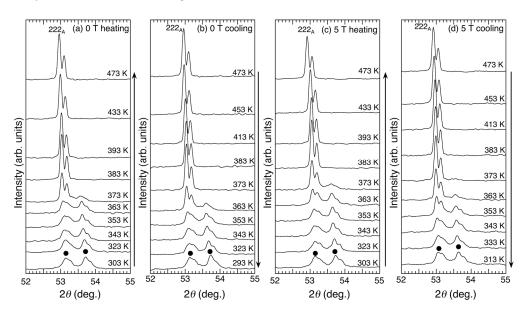

Figure 4. XRD patterns of $Ni_{46.4}Mn_{38.8}In_{12.8}Co_{2.0}$ film in (**a**) heating in a zero field, (**b**) cooling in a zero field, (**c**) heating in 5 T, and (**d**) cooling in 5 T. hkl_P indicates the Miller indices of the $L2_1$ structure (parent phase). The closed circles were the diffraction peaks derived to the martensitic phase.
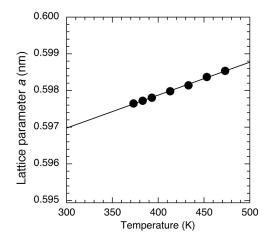

Figure 5. Lattice parameter a in the parent phase of $Ni_{46.4}Mn_{38.8}In_{12.8}Co_{2.0}$ film as a function of temperature. The solid line was obtained by the least-squares calculations.
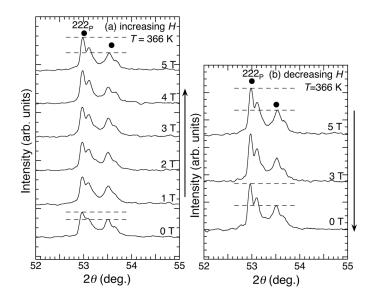
Figure 6. Isothermal XRD patterns at fixed temperature of 366 K with (**a**) increasing $\mu_0 H$ from 0 to 5 T, and (**b**) decreasing $\mu_0 H$ to 0 T. 220_P indicates the Miller indices of the $L2_1$ structure (parent phase). The closed circles are the diffraction peaks belonging to the martensitic phase. The broken lines indicate the differences in intensities between the two diffraction patterns.
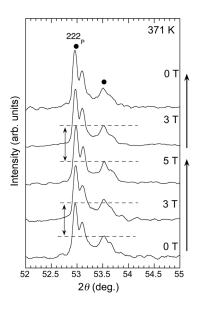

Figure 7. Isothermal XRD patterns at fixed temperature of 371 K. 220_P indicates the Miller indices of the $L2_1$ structure (parent phase). The closed circles are the diffraction peaks belonging to the martensitic phase. The broken lines indicate I_{P-M}.

In this study, the application of $\mu_0 H = 5$ T was not enough to finish the reverse transformation completely at 366 K. From the *M–T* curve, the extrapolated magnetization of the P-phase was considered to be 40 A·m^2/kg at 366 K. Herein, when metamagnetic transition is seen, discontinuous change in magnetization appeared. In this study, this discontinuous change was approximated by a linear relation. If *M* increased linearly during metamagnetic transition of the films, the extrapolated line for *M–H* curves at 366 K for $\mu_0 H > 4$ T in Figure 2 reached 40 A·m^2/kg at $\mu_0 H \sim 36$ T. Thus, $\mu_0 H \sim 36$ T is required to observe the complete transformation of the film at 366 K.
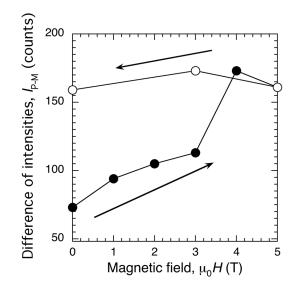
Figure 8. Differences between the peak intensity at $2\theta \sim 53°$ (martensitic + parent phases) and $53.5°$ (martensitic phase), I_{P-M}, as a function of magnetic field. The data was obtained by isothermal diffraction patterns at 366 K, which is shown in Figure 6.

4. Conclusions

The in situ observation of martensitic transformations for $Ni_{46.4}Mn_{38.8}In_{12.8}Co_{2.0}$ MSM film was performed by high field X-ray diffraction measurements in magnetic fields up to 5 T and in the temperature region from 298 to 473 K. The prepared films show the preferred orientation along (111) plane of the $L2_1$ structure at 473 K. A magnetic field-induced reverse transformation from M- to P-phase with $L2_1$ structure was observed at 366 K, which was just around A_s. The reverse transformation induced by magnetic fields was directly observed by in situ HF-XRD technique. Combining the change of the XRD patterns and the magnetization jumps, it was found that the metamagnetic transition of Ni-Co-Mn-In film is actually related to the martensitic transformation.

Author Contributions: Yoshifuru Mitsui performed the experiments and wrote the paper. Keiichi Koyama designed the experiments; Makoto Ohtsuka and Ryosuke Kainuma prepared the sample. Rie Y. Umetsu analyzed the data; Kazuo Watanabe supervised the HF-XRD experiments.

Conflicts of Interest: The authors declare no conflict of interest.

References

1. Ullakko, K.; Huang, J.K.; Kantner, C.; O'Handley, R.C.; Kokorin, V.V. Large magnetic-field-induced strains in Ni_2MnGa single crystals. *Appl. Phys. Lett.* **1996**, *69*, 1966–1968. [CrossRef]
2. Ullakko, K.; Huang, J.K.; Kokorin, V.V.; O'Handley, R.C. Magnetically controlled shape memory effect in Ni_2MnGa intermetallics. *Scr. Mater.* **1997**, *36*, 1133–1138. [CrossRef]
3. Vasil'ev, A.N.; Bozhko, A.D.; Khvailo, V.V.; Dikshtein, I.E.; Shavrov, V.G.; Buchelnikov, V.D.; Matsumoto, M.; Suzuki, S.; Takagi, T.; Tani, J. Structural and magnetic phase transitions in shape-memory alloys $Ni_{2+x}Mn_{1-x}Ga$. *Phys. Rev. B* **1999**, *59*, 1113–1120. [CrossRef]
4. Xu, X.; Nagasako, M.; Ito, W.; Umetsu, R.Y.; Kanomata, T.; Kainuma, R. Magnetic properties and phase diagram of $Ni_{50}Mn_{50-x}Ga_x$ ferromagnetic shape memory alloys. *Acta Mater.* **2013**, *61*, 6712–6723. [CrossRef]
5. Sutou, Y.; Imano, Y.; Koeda, N.; Omori, T.; Kainuma, R.; Ishida, K.; Oikawa, K. Magnetic and martensitic transformation of NiMnX (X = In, Sn, Sb) ferromagnetic shape memory alloys. *Appl. Phys. Lett.* **2004**, *85*, 4358–4360. [CrossRef]

6. Khovaylo, V.V.; Kanomata, T.; Tanaka, T.; Nakashima, M.; Amako, Y.; Kainuma, R.; Umetsu, R.Y.; Morito, H.; Miki, H. Magnetic properties of $Ni_{50}Mn_{34.8}In_{15.2}$ probed by Mössbauer spectroscopy. *Phys. Rev. B* **2009**, *80*, 144409. [CrossRef]

7. Umetsu, R.Y.; Sano, K.; Fukushima, K.; Kanomata, T.; Taniguchi, Y.; Amako, Y.; Kainuma, R. Mössbauer spectroscopy studies on magnetic properties for [57]Fe-substituted Ni-Mn-Sn metamagnetic shape memory alloys. *Metals* **2013**, *3*, 225–236. [CrossRef]

8. Kainuma, R.; Imano, Y.; Ito, W.; Sutou, Y.; Morito, H.; Okamoto, S.; Kitakami, O.; Oikawa, K.; Fujita, A.; Kanomata, T.; et al. Magnetic-field-induced shape recovery by reverse phase transformation. *Nature* **2006**, *439*, 957–960. [CrossRef] [PubMed]

9. Kainuma, R.; Imano, Y.; Ito, W.; Morito, H.; Sutou, Y.; Oikawa, K.; Fujita, A.; Ishida, K.; Okamoto, S.; Kitakami, O.; et al. Metamagnetic shape memory effect in a Heusler-type $Ni_{43}Co_7Mn_{39}Sn_{11}$ polycrystalline alloy. *Appl. Phys. Lett.* **2006**, *88*, 192513. [CrossRef]

10. Ito, W.; Imano, Y.; Kainuma, R.; Sutou, Y.; Oikawa, K.; Ishida, K. Martensitic and Magnetic transformation behaviors in Heusler-Type NiMnIn and NiCoMnIn metamagnetic shape memory alloys. *Metall. Mater. Trans. A* **2007**, *38A*, 759–766. [CrossRef]

11. Wang, Y.D.; Ren, Y.; Huang, E.W.; Nie, Z.H.; Wang, G. Direct evidence on magnetic-field-induced phase transition in a NiCoMnIn ferromagnetic shape memory alloy under a stress field. *Appl. Phys. Lett.* **2007**, *90*, 101917. [CrossRef]

12. Kohl, M.; Brugger, D.; Ohtsuka, M.; Takagi, T. A novel actuation mechanism on the basis of ferromagnetic SMA thin films. *Sens. Actuators A* **2004**, *114*, 445–450. [CrossRef]

13. Kohl, M.; Krevet, B.; Ohtsuka, M.; Brugger, D.; Liu, Y. Ferromagnetic shape memory actuators. *Mater. Trans.* **2006**, *47*, 639–644.

14. Rumpf, H.; Craciunescu, C.M.; Modrow, H.; Olimov, H.M.; Quandt, E.; Wuttig, M. Successive occurrence of ferromagnetic and shape memory properties during crystallization of NiMnGa freestanding films. *J. Magn. Magn. Mater.* **2006**, *302*, 421–428. [CrossRef]

15. Liu, J.; Scheerbaum, N.; Hinz, D.; Gutfleisch, O. Magnetostructural transformation in Ni-Mn-In-Co ribbons. *Appl. Phys. Lett.* **2008**, *92*, 162509. [CrossRef]

16. Rios, S.; Karaman, I.; Zhang, X. Crystallization and high temperature shape memory behavior of sputter-deposited NiMnCoIn thin films. *Appl. Phys. Lett.* **2010**, *96*, 173102. [CrossRef]

17. Gueltig, M.; Ossmer, H.; Ohtsuka, M.; Miki, H.; Tsuchiya, K.; Takagi, T.; Kohl, M. High frequency thermal energy harvesting using magnetic shape memory films. *Adv. Energy Mater.* **2014**, *4*, 1400751. [CrossRef]

18. Miki, H.; Tsuchiya, K.; Ohtsuka, M.; Gueltig, M.; Kohl, M.; Takagi, T. Structural and magnetic properties of magnetic shape memory alloys on Ni-Mn-Co-In self-standing films. In *Advances in Shape Memory Materials*; Springer: Basel, Switzerland, 2017; Volume 73, pp. 149–160.

19. Pecharsky, V.K.; Holm, A.P.; Gschneider, K.A., Jr.; Rink, R. Massive magnetic-field-induced structural transformation in Gd_5Ge_4 and the nature of the giant magnetocaloric effect. *Phys. Rev. Lett.* **2003**, *91*, 197204. [CrossRef] [PubMed]

20. Fujita, A.; Fukamichi, K.; Koyama, K.; Watanabe, K. X-ray diffraction study in high magnetic fields of magnetovolume effect in itinerant-electron metamagnetic $La(Fe_{0.88}Si_{0.12})_{13}$ compound. *J. Appl. Phys.* **2004**, *95*, 6687–6689. [CrossRef]

21. Koyama, K.; Kanomata, T.; Matsukawa, T.; Watanabe, K. Magnetic field effect on structural property of $MnFeP_{0.5}As_{0.5}$. *Mater. Trans.* **2005**, *46*, 1753–1756. [CrossRef]

22. Ma, Y.; Awaji, S.; Watanabe, K.; Matsumoto, M.; Kobayashi, N. Effect of high magnetic field on the two-step martensitic-phase transition in Ni_2MnGa. *Appl. Phys. Lett.* **2000**, *76*, 37–39. [CrossRef]

23. Koyama, K.; Watanabe, K.; Kanomata, T.; Kainuma, R.; Oikawa, K.; Ishida, K. Observation of field-induced reverse transformation in ferromagnetic shape memory alloy $Ni_{50}Mn_{36}Sn_{14}$. *Appl. Phys. Lett.* **2006**, *88*, 132505. [CrossRef]

24. Ito, W.; Ito, K.; Umetsu, R.Y.; Kainuma, R.; Koyama, K.; Watanabe, K.; Fujita, A.; Oikawa, K.; Ishida, K.; Kanomata, T. Kinetic arrest of martensitic transformation in the NiCoMnIn metamagnetic shape memory alloy. *Appl. Phys. Lett.* **2008**, *92*, 021908. [CrossRef]

25. Mitsui, Y.; Koyama, K.; Watanabe, K. X-ray diffraction measurements in high magnetic fields and at high temperatures. *Sci. Technol. Adv. Mater.* **2009**, *9*, 014612. [CrossRef] [PubMed]
26. Mitsui, Y.; Koyama, K.; Ito, W.; Umetsu, R.Y.; Kainuma, R.; Watanabe, K. Observation of reverse transformation in metamagnetic shape memory alloy $Ni_{40}Co_{10}Mn_{34}Al_{16}$ by high-field X-Ray diffraction measurements. *Mater. Trans.* **2010**, *51*, 1648–1650. [CrossRef]